Effective automated method for detection and suppression of muscle artefacts from single-channel EEG signal

Manali Saini[1], *Udit Satija*[2] ✉, *Madhur Deo Upadhayay*[1]

[1]*Department of Electrical Engineering, Shiv Nadar University, Greater Noida, UP 201314, India*
[2]*Department of Electrical Engineering, Indian Institute of Technology Patna, Bihta, Patna 801103, Bihar, India*
✉ *E-mail: us11@iitbbs.ac.in*

Published in Healthcare Technology Letters; Received on 7th August 2019; Revised on 9th October 2019; Accepted on 19th December 2019

This Letter proposes an automated method for the detection and suppression of muscle artefacts (MAs) in the single-channel electroencephalogram (EEG) signal based on variational mode decomposition (VMD) and zero crossings count threshold criterion without the use of reference electromyogram (EMG). The proposed method involves three major steps: decomposition of the input EEG signal into two modes using VMD; detection of MAs based on zero crossings count thresholding in the second mode; retention of the first mode as MAs-free EEG signal only after detection of MAs in the second mode. The authors evaluate the robustness of the proposed method on a variety of EEG and EMG signals taken from publicly available databases, including Mendeley database, epileptic Bonn database and EEG during mental arithmetic tasks database (EEGMAT). Evaluation results using different objective performance metrics depict the superiority of the proposed method as compared to existing methods while preserving the clinical features of the reconstructed EEG signal.

1. Introduction: Electroencephalogram (EEG) represents the electrical activity of the brain [1]. EEG signal can be recorded using surface electrodes from the scalp and its amplitude is in microvolts [1]. Since it is a non-invasive signal acquisition technique, it finds numerous applications in the field of neuroscience, diagnosis of neurological disorders, brain–computer interface, cognitive science, psychology and physio-psychological research [1]. However, it is often corrupted by different artefacts such as ocular artefacts (eye blinks), muscle artefacts (biting, chewing, etc.), cardiac activity [1, 2]. These artefacts represent the electrical activities of regions other than the brain [1]. Muscle artefacts (MAs) are the most frequent artefacts which are introduced in the EEG signal due to the contraction and relaxation of muscles. MA considerably distorts activities of α and β subbands of EEG signals. However, it almost impacts all EEG local subbands due to its broad-spectrum, starting as low as 2 Hz [3]. Generally, MAs have a high amplitude, broad-spectrum, and high sensitivity as compared to EEG signals [4]. However, these artefacts are difficult to standardise as the spectral and topographical characteristics of MAs vary based on the magnitude and particular type of muscle contraction, and different individuals [3, 5]. MAs are more difficult to suppress without distorting the clinical features of the EEG signal as compared to OAs and cardiac artefacts [4, 6]. Therefore, many filtering and source separation techniques have been presented for suppressing the MAs.

1.1. Related work: Various methods have been proposed to suppress MAs based on digital and adaptive filtering [7], regression [8], blind source separation (BSS) [2, 9–12], wavelet and signal decomposition [4, 13–16]. Since digital filtering based methods use low-pass filters in order to suppress the high-frequency content from the MA-contaminated EEG data, EEG content is also distorted in the filtering process due to spectral overlap between EEG and MAs [4, 5]. In [7], the adaptive filter has been used to remove MAs and EOG from EEG based on the least mean square algorithm. However, it requires a reference EOG and EMG signal, which may not be always available. A regression-based surface MAs correction in the EEG signal has been proposed in [8]. Although it is computationally simple, it predicts MAs only in the band 51–69 Hz in regression analysis, which may not always be correct and needs to be changed depending upon the MAs. In [2, 9, 17], independent component analysis (ICA) has been used to suppress the MA components by discarding the independent components (ICs) containing MAs. However, the rejection of ICs directly can result in the loss of some of the EEG components captured in those ICs. Furthermore, several assumptions in the ICA-based methods, such as the independence of sources along with non-Gaussian distributions, the same number of sources and sensors, the mixtures being linear combinations of sources limit the reliability of ICA-based method in the suppression of MAs in single-channel EEG signal. Another BSS technique, namely canonical correlation analysis (CCA), has been applied in [10–12] for the segregation of MAs and EEG sources based on the assumption of mutually uncorrelated sources while maximally autocorrelated. Although CCA is able to segregate MAs from the brain activity due to low autocorrelation of EMG in comparison with EEG [10], the selection of robust threshold in autocorrelation is challenging for a large dataset. Furthermore, ICA and CCA based methods require multichannel EEG data for the separation of EEG and MA components [13]. Due to the inclination towards ambulatory EEG based systems, there is a surge of interest recently towards developing light-weight, less complex systems with a limited number of EEG channels or single channel [13]. Therefore, few single-channel artefact rejection techniques have been proposed for the suppression of MAs. Davies and James [18] proposed the use of single-channel ICA (SC-ICA) to decompose a single-channel EEG into ICs. However, it incurs the problem of strict assumptions of stationary sources and disjointness in spectral-domain [13, 19]. A discrete wavelet transform (DWT)-based denoising algorithm namely 'SURE' with thresholding, has been proposed for MAs removal from ictal EEG recordings [20]. However, the performance of this method is significantly degraded under low signal-to-noise ratio (SNR) due to smaller values of wavelet coefficients. In [21], wavelet denoising has been used for removing motion artefacts for functional near-infrared spectroscopy, but it fails to show improvement for the databases without known motion. Some of the MAs removal techniques exploit the use of decomposition techniques (such as wavelet transform [14], empirical mode decomposition (EMD) and ensemble EMD (EEMD) [4, 13]) for generating multi-channel EEG data from single-channel EEG to further enable the application of BSS methods (such as ICA, CCA, and multiset CCA (MCCA)) [4, 15, 16].

Most of the MAs suppression methods exploit BSS methods for separating the MAs information from the acquired multi-channel

EEG signals. However, the orthogonality condition for EEG signals and MAs may not hold true, which is most commonly assumed in the ICA techniques. Though some of the improved ICA techniques are effective in suppressing the MAs by discarding independent component(s) (IC(s)), the need for simultaneously acquired multi-channel EEG signals limits their applicability in portable and ambulatory EEG applications. In addition, the improper identification of ICs in the presence of several EEG artefacts can result in the loss of important clinical information in the EEG signal.

1.2. Objective and major contributions: Literature studies demonstrate that most of the existing MAs suppression methods need multi-channel EEG signals to exploit BSS techniques (ICA and CCA), which affects the patient's convenience. Also, many of the existing techniques demand the reference EMG signal for filtering out the MAs signal which may not be always available. As mentioned earlier, few single-channel MAs suppression techniques have been proposed based on two-stage processing: generate multi-channel EEG signals by using decomposition techniques; and extraction of different sources using the decomposed modes. However, these techniques are not only quite computationally complex but also employ visual inference to discard the extracted component with MAs. Therefore, there is a need to develop an effective automated method that not only preserves the clinically valuable information in the reconstructed EEG signal but is also computationally less complex.

This Letter proposes a novel and effective method to suppress MAs based on variational mode decomposition (VMD) without the use of any reference signal. The proposed method works in three steps: decomposition of the input EEG signal into two modes using VMD; rejection of MA components in the second mode based on a proposed zero-crossings count (zc) feature; retention of the first mode as MAs-free EEG signal only after detection of the presence of MAs in the second mode. Evaluation results depict that the proposed method not only suppresses MAs with minimal loss of clinically valuable features but is also computationally very simple. Finally, the major contributions of the Letter can be summarised as follows:

- Investigation of VMD with specific parameters for extracting the MAs from EEG signals in one of the decomposed modes.
- Exploring the zero-crossings count feature for the detection of MAs in modes.
- Proposed MAs detection and suppression in single-channel EEG signal without the use of reference EMG signal, unlike many existing multi-channel EEG signal based MAs suppression methods and/or MAs suppression with the use of reference EMG signals.
- Demonstration of comparative analysis of detecting and suppressing MAs using the proposed method and recent existing MAs-removal methods evaluated on various publicly available databases.
- Demonstration of the robustness of the proposed method in detecting and suppressing MAs for varying processing lengths of EEG signal and for inter-variability among subjects from different databases using different performance metrics.
- Detection and suppression of MAs from EEG signal with low computational time complexity.

The rest of the Letter is organised as follows: Section 2 describes the major components of the proposed method. Section 3 discusses the performance results obtained on different EEG signals taken from various publicly available databases. Section 4 concludes the Letter.

2. Proposed VMD-based MAs removal method: The flow diagram for the proposed MAs suppression method based on VMD is shown in Fig. 1. The proposed method consists of three major stages: decomposition of the original EEG signal into two modes using VMD; rejection of the second mode containing MAs based on zero crossings count feature; retention of the first mode as MAs-free EEG signal only after detection of MAs. In this section, we present a brief overview of VMD and its application in the suppression of MAs.

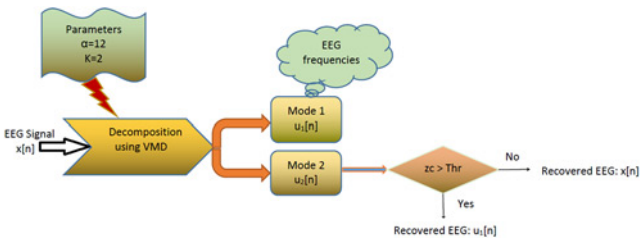

Fig. 1 *Flow diagram for the proposed MAs suppression method*

2.1. Variational mode decomposition: VMD is a non-recursive decomposition of a real-valued signal $x(t)$ into a distinct bandlimited M number of modes (each with different centre frequency) [22–24]. Each mode is a combination of amplitude modulated and frequency modulated (AM–FM) signal which can be represented as

$$v(t) = a(t)\cos\big(\phi(t)\big) \tag{1}$$

where $\phi(t)$ is a non-decreasing phase and $a(t)$ is the non-negative envelope of the $v(t)$.

VMD formulates the problem of estimating the bandwidth of each mode as the following constrained variational problem:

$$\min_{\{v_m\},\{\omega_m\}} \left\{ \sum_m \left\| \partial_t \left[\left(\delta(t) + \frac{j}{\pi t} \right) * v_m(t) \right] \mathrm{e}^{-j\omega_m t} \right\|_2^2 \right\} \quad \text{s.t.} \quad \sum_{m=1}^{M} v_m(t) = x(t) \tag{2}$$

where $v_m(t)$ represents the mth mode, ω_m represents its centre frequency, $x(t)$ represents the signal to be decomposed, $\delta(t)$ is the impulse signal and ∂_t is the gradient with respect to t. This constrained problem is converted into the unconstrained problem by making use of the Lagrange multiplier and quadratic penalty term, thereby introducing an augmented Lagrange multiplier [22].

The solution to the above-constrained optimisation problem is obtained in a sequence of iterations using the alternate direction method of multipliers and the following update equations are obtained for mode and centre frequency [22]:

$$\hat{v}_m^{n+1}(\omega) = \frac{\hat{x}(\omega) - \sum_{j \neq m} \hat{v}_j^n(\omega) + \left(\hat{\lambda}^n(\omega)/2\right)}{1 + 2\alpha\left(\omega - \omega_m^n\right)^2}. \tag{3}$$

Here, the modes are directly updated in the spectral domain using Wiener filtering with centre frequency of ω_m. $\hat{v}(\omega)$ denotes the mode spectrum, n is the iteration number and α is the data fidelity parameter

$$\omega_m^{n+1} = \frac{\int_0^\infty \omega \left|\hat{v}_m(\omega)\right|^2 \mathrm{d}\omega}{\int_0^\infty \left|\hat{v}_m(\omega)\right|^2 \mathrm{d}\omega}. \tag{4}$$

The centre frequency is updated as the centre of gravity of the corresponding mode's power spectrum. The Lagrangian multiplier is

doi: 10.1049/htl.2019.0053

1: Initialize $\hat{v}_m, \omega_m, \hat{\lambda}, n \to 0$
2: $n \leftarrow n+1$
3: Update $\hat{v}_m$
$\hat{v}_m^{n+1}(\omega) = \frac{\hat{x}(\omega) - \sum_{j \neq m} \hat{v}_j(\omega) + (\hat{\lambda}(\omega)/2)}{1+2\alpha(\omega-\omega_m)^2}$
4: Update ω_m
$\omega_m^{n+1} = \frac{\int_0^\infty \omega |\hat{v}_m(\omega)|^2 d\omega}{\int_0^\infty |\hat{v}_m(\omega)|^2 d\omega}$
5: Update $\hat{\lambda}^{n+1}(\omega) \leftarrow \hat{\lambda}^n(\omega) + \zeta(\hat{x}(\omega) - \sum_m \hat{v}_m^{n+1}(\omega))$ until convergence $\sum_m ||\hat{v}_m^{n+1} - \hat{v}_m^n||_2^2 < \epsilon$, Here, $\epsilon = 10^{-6}$.

Fig. 2 *Algorithm 1: Pseudocode for VMD*

updated in the unconstrained problem as

$$\hat{\lambda}^{n+1} = \hat{\lambda}^n + \zeta\left(\hat{x} - \sum_m \hat{v}_m^{n+1}\right), \tag{5}$$

until $\sum_k \|\hat{v}_m^{n+1} - \hat{v}_m^n\|_2^2 \leq \epsilon$. λ denotes the Lagrangian multiplier. The algorithm for VMD is summarised in Fig. 2.

2.2. Utilisation of VMD for suppression of MAs: In this section, we propose the use of VMD to effectively suppress MAs from the EEG signal by adjusting specific VMD parameters. The choice of two design parameters: data fidelity parameter (α) and the number of modes (M) plays a major role in effectively removing MAs from the EEG signal. The value of α decides the bandwidth allowed in each mode and the number of modes should be selected in such a way that the energy is distributed across the modes appropriately. In this work, the parameters are chosen as $\alpha = 12$ and $M = 2$ after rigorous experimental assessment. Let $x[n]$ denote a single-channel EEG signal. The decomposed modes of $x[n]$ using VMD with the aforementioned parameters can be represented as

$$v_j\{n, f, \omega\} = \text{VMD}\{x[n]\}, \tag{6}$$

where $j = 1, 2, ..., L$. The decomposed modes of $x[n]$ are shown in Fig. 3. It can be observed from the figure that the first mode

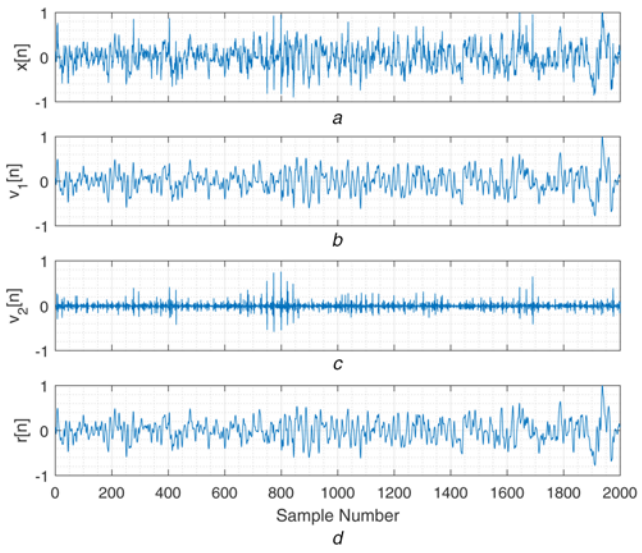

Fig. 3 *Illustrates the original EEG signal decomposition and reconstruction using VMD*
a Input EEG signal taken from EEGMAT (EEG during mental arithmetic tasks) database contaminated with MAs
b, *c* Decomposed modes using VMD (the first mode illustrates the information of MA-free EEG)
d Reconstructed EEG signal

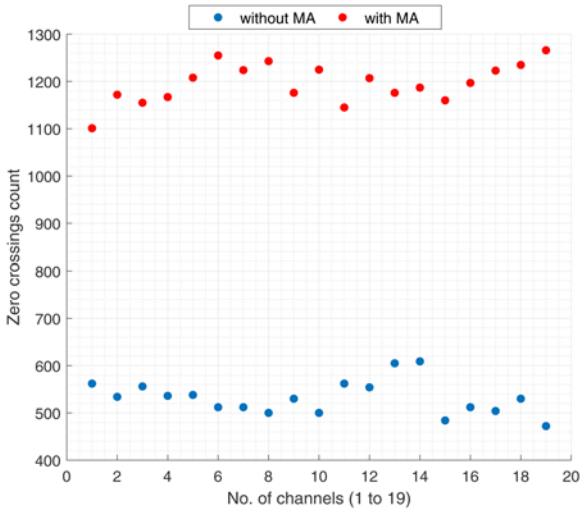

Fig. 4 *Illustrates the zc count feature in the second mode of decomposed clean and MAs-contaminated EEG signal taken from one subject (with 19 channels) of the Mendeley database*

$v_1[n]$ effectively captures true EEG information. However, the information of MAs is captured in the second mode $v_2[n]$.

In this Letter, we propose the zero-crossings count (zc) feature to detect the presence of MAs in the second mode $v_2[n]$ which can be computed as

$$\text{zc} = \sum_{n=1}^{L} g[n], \tag{7}$$

where $g[n]$ can be computed as

$$g[n] = \begin{cases} 1 & (\text{sign}(v_2[n]) > 0) \&\& (\text{sign}(v_2[n+1]) < 0) \\ 0 & \text{otherwise} \end{cases}, \tag{8}$$

and, L denotes the size of zc.

Fig. 4 depicts the zc feature. It can be observed from the figure that the values of zc feature in the second mode are higher in the presence of MAs as compared to the MAs-free EEG signal. Then, the zc feature is compared with a predefined threshold for the detection of MAs in the second mode. The predefined threshold is chosen as the mean value of both the decision boundaries shown in Fig. 4. Once the MAs are detected in the second mode, the first mode is chosen as an MAs-free EEG signal.

3. Results and discussion: In this section, we evaluate the performance of the proposed method on EEG signals taken from different publicly available databases. In this section, we first describe different test databases and performance metrics. Then, simulation results are presented to demonstrate the effectiveness of the proposed method in suppressing MAs from single-channel EEG.

3.1. Test databases and performance metrics: The proposed method has been tested on EEG and EMG signals taken from five publicly available databases including Mendeley database [25], epileptic Bonn database (set 'Z') [26], EEG during mental arithmetic tasks (EEGMAT) [27], examples of electromyograms [27] and cerebral vasoregulation in elderly with stroke (CVES) database [27]. Mendeley database consists of clean EEG recordings from various subjects, each with 19 electrodes positioned using a 10–20 electrode placement system. The data is recorded at a sampling rate of 200 Hz. Epileptic Bonn database consists of five

different sets of databases denoted as sets A, B, C, D and E with Z, O, N, F and S folders, respectively, where Z and O contain EEG recordings of five healthy subjects with eyes open and closed, respectively. N and F contain inter-ictal recordings from seizure patients and S represents the seizure-EEG signals. Each set consists of 23.6 s recording of 100 signals sampled at 173.61 Hz. In this work, we used only the set Z. EEGMAT database consists of EEG and ECG signals recorded from 36 subjects before and during the performance of mental arithmetic tasks. The signals are recorded at the sampling frequency of 500 Hz using a 23-channel system. Examples of electromyograms consist of three clean EMG (MAs) signals recorded from healthy subjects and patients with myopathy and neuropathy. The CVES database consists of clean EMG signals along with blood pressure (BP), sit-stand, head-up tilt, etc. In this work, we generate various realisations of MAs-contaminated EEG data by mixing clean EEG signals and EMG signals randomly from all records of these databases after re-sampling at the rate of 200 Hz.

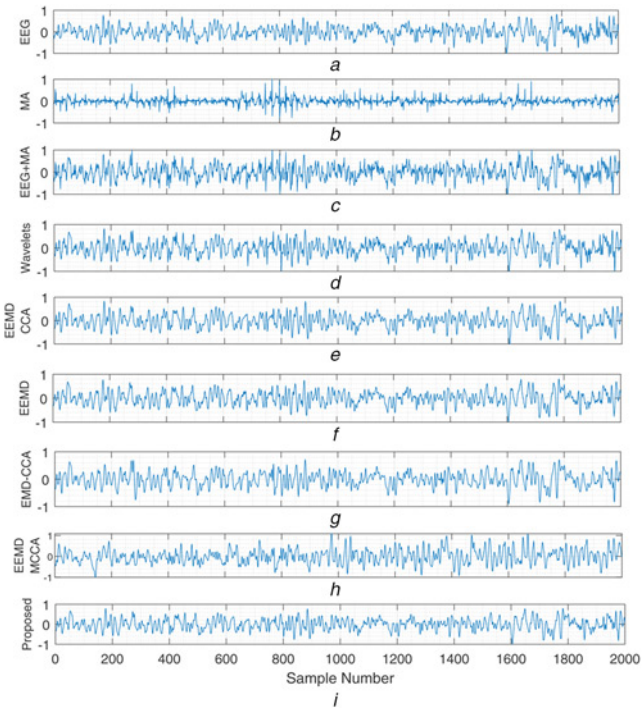

Fig. 5 *Comparative denoising results for the existing methods and proposed method*
a Original artefact-free EEG signal taken from EEGMAT database
b EMG signal taken from examples of electromyograms database
c MAs-corrupted EEG signal
d Reconstructed EEG signal using wavelet [21]
e Reconstructed EEG signal using EEMD-CCA [16]
f Reconstructed EEG signal using EEMD [13]
g Reconstructed EEG signal using EMD-CCA [16]
h Reconstructed EEG signal using EEMD-MCCA [4]
i Reconstructed EEG signal using proposed method

In this work, different performance metrics including, percentage root mean square difference (PRD), root mean square error (RMSE), signal-to-noise ratio (SNR), mean absolute error (MAE), correlation coefficient (CC) and time complexity (TC), have been used to perform objective assessment of the reconstructed signal quality after MAs suppression. Let $r[n]$ denote the reconstructed EEG signal after MAs suppression. The error between original and reconstructed signals can be given as $e[n] = x[n] - r[n]$. The performance metrics can be calculated as

$$\mathrm{PRD} = \sqrt{\frac{\sum_{n=1}^{N} e[n]^2}{\sum_{n=1}^{N} (x[n] - M_x)^2}} \tag{9}$$

$$\mathrm{RMSE} = \sqrt{\frac{\sum_{n=1}^{N} \left(e[n]^2\right)}{N}} \tag{10}$$

$$\mathrm{SNR} = 10\ \log_{10} \frac{(1/N)\sum_{n=1}^{N} |x[n]|^2}{(1/N)\sum_{n=1}^{N} |r[n] - x[n]|^2} \tag{11}$$

$$\mathrm{MAE} = \frac{\sum_{n=1}^{N} |e[n]|}{N} \tag{12}$$

$$CC = \frac{\sum_{n=1}^{N} (x[n] - M_x)\big(r[n] - M_r\big)}{\sqrt{\sum_{n=1}^{N} \big(x[n] - M_x\big)^2}\sqrt{\sum_{n=1}^{N} \big(r[n] - M_r\big)^2}} \tag{13}$$

where M_x and M_r denote the mean of $x[n]$ and $r[n]$, respectively, and N represents the number of samples in the EEG signal. TC denotes the execution time in seconds.

Table 1 Comparison results for proposed and existing MAs suppression methods (mean (standard deviation))

Method	Database	PRD	RMSE	SNR (dB)	MAE	CC	TC (s)
EEMD-CCA [16]	Mendeley	45.00 (8.12)	0.11 (0.006)	7.20 (1.30)	0.08 (0.005)	0.90 (0.03)	1.20 (0.60)
	Epileptic Bonn (Set Z)	39.00 (4.49)	0.11 (0.006)	8.20 (1.10)	0.08 (0.006)	0.93 (0.01)	1.10 (0.50)
	EEGMAT	41.36 (8.21)	0.11 (0.008)	7.80 (1.50)	0.08 (0.007)	0.92 (0.03)	1.60 (0.30)
EEMD [13]	Mendeley	43.61 (7.61)	0.11 (0.006)	7.46 (1.30)	0.08 (0.006)	0.90 (0.03)	1.00 (0.40)
	Bonn	38.01 (4.61)	0.10 (0.004)	8.44 (1.00)	0.08 (0.004)	0.93 (0.01)	0.90 (0.30)
	EEGMAT	39.81 (8.01)	0.11 (0.007)	8.13 (1.50)	0.08 (0.006)	0.92 (0.03)	0.90 (0.30)
EMD-CCA [16]	Mendeley	59.56 (7.81)	0.15 (0.020)	4.46 (1.10)	0.11 (0.010)	0.81 (0.05)	0.25 (0.10)
	Epileptic Bonn (Set Z)	53.81 (7.71)	0.15 (0.020)	5.45 (1.20)	0.10 (0.010)	0.85 (0.05)	0.30 (0.20)
	EEGMAT	52.21 (8.97)	0.14 (0.020)	5.76 (1.40)	0.10 (0.010)	0.85 (0.06)	0.30 (0.20)
Wavelet Denoising [21]	Mendeley	45.51 (7.61)	0.11 (0.001)	7.10 (1.20)	0.08 (0.001)	0.90 (0.03)	0.20 (0.10)
	Epileptic Bonn (Set Z)	41.52 (5.32)	0.11 (0.002)	7.70 (1.10)	0.08 (0.002)	0.92 (0.02)	0.63 (0.10)
	EEGMAT	42.52 (8.62)	0.11 (0.002)	7.60 (1.50)	0.08 (0.002)	0.91 (0.03)	0.20 (0.10)
EEMD-MCCA [4]	Mendeley	44.78 (7.72)	0.11 (0.006)	7.26 (1.20)	0.08 (0.005)	0.90 (0.30)	1.50 (0.40)
	Epileptic Bonn (Set Z)	38.94 (5.21)	0.11 (0.007)	8.26 (1.10)	0.08 (0.006)	0.93 (0.10)	1.60 (0.30)
	EEGMAT	41.32 (7.83)	0.11 (0.009)	7.81 (1.40)	0.08 (0.008)	0.92 (0.30)	1.50 (0.40)
proposed method	Mendeley	41.46 (7.44)	0.10 (0.008)	8.00 (1.30)	0.07 (0.007)	0.92 (0.03)	0.10 (0.10)
	Epileptic Bonn (Set Z)	36.13 (4.51)	0.09 (0.002)	9.00 (1.00)	0.07 (0.002)	0.95 (0.01)	0.10 (0.05)
	EEGMAT	37.74 (8.11)	0.10 (0.010)	8.62 (1.60)	0.07 (0.009)	0.93 (0.03)	0.10 (0.10)

doi: 10.1049/htl.2019.0053

Table 2 Impact of processing EEG length for the proposed method

Time, s	Database	PRD	SNR (dB)	MAE	CC	TC (s)	ZC (EEG)	ZC (MAs)
5	Mendeley	42.00	7.64	0.08	0.91	0.06	266 (36.31)	595 (77.88)
	Bonn (Set Z)	37.88	8.50	0.08	0.93	0.07	195 (54.74)	650 (15.14)
	EEGMAT	39.60	8.18	0.08	0.92	0.05	242 (48.99)	583 (70.00)
10	Mendeley	41.43	8.00	0.07	0.92	0.10	525 (70.42)	1164 (157.57)
	Bonn (Set Z)	36.00	9.00	0.07	0.94	0.10	384 (96.21)	1270 (25.58)
	EEGMAT	37.89	8.62	0.07	0.93	0.10	485 (92.42)	1150 (107.97)
15	Mendeley	42.79	7.65	0.07	0.91	0.20	783 (105.16)	1729 (224.03)
	Bonn (Set Z)	37.84	8.50	0.07	0.93	0.15	567 (104.49)	1886 (34.99)
	EEGMAT	40.18	8.07	0.07	0.92	0.20	732 (134.21)	1709 (157.19)
20	Mendeley	43.64	7.45	0.07	0.91	0.25	1038 (142.25)	2376 (235.29)
	Bonn (Set Z)	38.97	8.24	0.07	0.93	0.30	750 (141.44)	2532 (41.12)
	EEGMAT	41.96	7.71	0.07	0.91	0.30	970 (181.37)	2326 (188.87)

3.2. Performance comparison: In this Letter, we first evaluate the performance of the proposed method in detecting the presence of MAs in the EEG signals. Results show that our proposed method achieves a Se of 100% in detecting all the MAs-corrupted EEG signals taken from all three databases. To present the efficacy of the proposed method, we implement some of the existing denoising methods such as EEMD [13], EEMD-CCA [16], EMD-CCA [16], EEMD-MCCA [4] and wavelet denoising [21] for suppressing MAs from the EEG signal. It can be seen from Fig. 5 that the proposed method outperforms the existing methods in suppressing the MAs. Comparison evaluation results in terms of objective performance metrics for the proposed method and existing methods are shown in Table 1. It can be seen from the table that the proposed method outperforms other existing methods in terms of performance metrics and is computationally simple. Also, it can be seen from the mean and standard deviation values that the proposed method is robust to the inter-variability among subjects in order to suppress MAs from EEG signals. We also analyse the impact of varying processing length of EEG signal on evaluation results for detection and suppression of MAs. Table 2 depicts the impact of processing EEG length on performance metrics and zero crossings count (ZC) feature (mean (standard deviation)). It can be seen that processing length of EEG signal of 10 s gives better deviation between the mean value of ZC (decision boundaries) in the case of MAs-free EEG signal and EEG signal contaminated with MAs for deciding a robust threshold for the detection of MAs. Also, it gives better MAs suppression in terms of different objective performance metrics. Based on the results, we can state that our proposed method can provide adequate EEG analysis in different ambulatory systems due to the effective suppression of MAs.

4. Conclusion: In this work, we proposed an effective automated method based on VMD to suppress MAs from the EEG signal in three steps. In the first step, VMD is used with specific parameters to decompose the original EEG signal into two modes. In the second step, detection of the presence of MAs is accomplished based on zero crossings count thresholding in the second decomposed mode. Finally, in order to get a MAs-free EEG signal, the first mode is retained only if the presence of MAs is detected in the second mode; otherwise, the original signal is considered as MAs-free signal. The proposed method has been tested on a variety of publicly available databases for various MAs-corrupted EEG signals of all subjects. Comparison results in terms of different performance metrics demonstrate that the proposed method can effectively suppress the MAs as compared to existing methods.

5 References

[1] Mannan M.M.N., Kamran M.A., Jeong M.Y.: 'Identification and removal of physiological artifacts from electroencephalogram signals: a review', *IEEE Access*, 2018, **6**, pp. 30630–30652

[2] Iriarte J., Urrestarazu E., Valencia M., *ET AL.*: 'Independent component analysis as a tool to eliminate artifacts in EEG: a quantitative study', *J. Clin. Neurophysiol.*, 2003, **20**, (4), pp. 249–257

[3] Urigüen J.A., Zapirain B.G.: 'EEG artifact removal-state-of-the-art and guidelines', *J. Neural Eng.*, 2015, **12**, (3), p. 031001

[4] Chen X., He C., Peng H.: 'Removal of muscle artifacts from single-channel EEG based on ensemble empirical mode decomposition and multi set canonical correlation analysis', *J. Appl. Math.*, 2014, pp. 1–10

[5] Goncharova I.I., McFarland D., Vaughan T., *ET AL.*: 'EMG contamination of EEG: spectral and topographical characteristics', *Clin. Neurophysiol.*, 2003, **114**, (9), pp. 1580–1593

[6] McMenamin B.W., Shackman A.J., Greischar L.L., *ET AL.*: 'Electromyogenic artifacts and electroencephalographic inferences revisited', *Neuroimage*, 2011, **54**, (1), pp. 4–9

[7] Mehrkanoon S., Moghavvemi M., Fariborzi H.: 'Real time ocular and facial muscle artifacts removal from EEG signals using LMS adaptive algorithm'. Int. Conf. on Intelligent and Advanced Systems, Kuala Lumpur, 2007, pp. 1245–1250

[8] Gasser T., Schuller J.C., Gasser U.S.: 'Correction of muscle artefacts in the EEG power spectrum', *Clin. Neurophysiol.*, 2005, **116**, (9), pp. 2044–2050

[9] Jung T.P., Humphries C., Lee T.W.: 'Extended ICA removes artifacts from electroencephalographic recordings'. In 'Advances in Neural Information Processing Systems', 1998, pp. 894–900

[10] Clercq W.D., Vergult A., Vanrumste B., *ET AL.*: 'Canonical correlation analysis applied to remove muscle artifacts from the electroencephalogram', *IEEE Trans. Biomed. Eng.*, 2006, **53**, (12), pp. 2583–2587

[11] Hallez H., Vergult A., Phlypo R.: 'Muscle and eye movement artifact removal prior to EEG source localization'. 2006 Int. Conf. of the IEEE Engineering in Medicine and Biology Society, New York, NY, 2006, pp. 1002–1005

[12] Gao J., Lin P., Yang Y., *ET AL.*: 'Online EMG artifacts removal from EEG based on blind source separation'. 2010 2nd Int. Asia Conf. on Informatics in Control, Automation and Robotics (CAR 2010), Wuhan, China, 2010, pp. 28–31

[13] Chen X., Liu A., Chiang J., *ET AL.*: 'Removing muscle artifacts from EEG data: multichannel or single-channel techniques?', *IEEE Sens. J.*, 2016, **16**, (7), pp. 1986–1997

[14] Mammone N., Foresta F.L., Morabito F.C.: 'Automatic artifact rejection from multichannel scalp EEG by wavelet ICA', *IEEE Sens. J.*, 2012, **12**, (3), pp. 533–542

[15] Mijovic B., Vos M.D., Gligorijevic I., *ET AL.*: 'Source separation from single-channel recordings by combining empirical-mode decomposition and independent component analysis', *IEEE Trans. Biomed. Eng.*, 2010, **57**, (9), pp. 2188–2196

[16] Sweeney K.T., McLoone S.F., Ward T.E.: 'The use of ensemble empirical mode decomposition with canonical correlation analysis as a novel artifact removal technique', *IEEE Trans. Biomed. Eng.*, 2013, **60**, (1), pp. 97–105

[17] Urrestarazu E., Iriarte J., Alegre M., *ET AL.*: 'Independent component analysis removing artifacts in Ictal recordings', *Epilepsia*, 2004, **45**, (9), pp. 1071–1078

[18] Davies M.E., James C.J.: 'Source separation using single channel ICA', *Signal Process.*, 2007, **87**, (8), pp. 1819–1832

[19] Djuwari D., Kumar D.K., Palaniswami M.: 'Limitations of ICA for artefact removal'. 2005 IEEE Engineering in Medicine and Biology 27th Annual Conf., Shanghai, 2005, pp. 4685–4688
[20] Safieddine D., Kachenoura A., Albera L., *ET AL.*: 'Removal of muscle artifact from EEG data: comparison between stochastic (ICA and CCA) and deterministic (EMD and wavelet-based) approaches', *EURASIP J. Adv. Signal Process.*, 2012, **2012**, (1), p. 127
[21] Robertson F.C., Douglas T.S., Meintjes E.M.: 'Motion artifact removal for functional near infrared spectroscopy: a comparison of methods', *IEEE Trans. Biomed. Eng.*, 2010, **57**, (6), pp. 1377–1387
[22] Dragomiretskiy K., Zosso D.: 'Variational mode decomposition', *IEEE Trans. Signal Process.*, 2014, **62**, (3), pp. 531–544
[23] Satija U., Trivedi N., Biswal G., *ET AL.*: 'Specific emitter identification based on variational mode decomposition and spectral features in single hop and relaying scenarios', *IEEE Trans. Inf. Forensics Secur.*, 2019, **14**, (3), pp. 581–591
[24] Dutta T., Satija U., Ramkumar B., *ET AL.*: 'A novel method for automatic modulation classification under non-Gaussian noise based on variational mode decomposition'. 2016 Twenty-Second National Conf. on Communication (NCC), Guwahati, 2016, pp. 1–6
[25] Klados M.A., Bamidis P.D.: 'A semi-simulated EEG/EOG dataset for the comparison of EOG artifact rejection techniques', *Data Brief*, 2016, **8**, pp. 1004–1006
[26] Andrzejak R.G., Lehnertz K., Mormann F., *ET AL.*: 'Indications of nonlinear deterministic and finite-dimensional structures in time series of brain electrical activity: dependence on recording region and brain state', *Phys. Rev. E*, 2001, **64**, (6), p. 061907
[27] Goldberger A., Amaral L., Glass L., *ET AL.*: 'Physiobank, physiotoolkit, and physionet: components of a new research resource for complex physiologic signals', *Circulation*, 2000, **101**, (23), pp. e215–e220

doi: 10.1049/htl.2019.0053